Journal of Microscopy, Vol. 199, Pt 3, September 2000, pp. 214–223.
Received 4 October 1999; accepted 28 March 2000

Temperature-controlled microscopy for imaging living cells: apparatus, thermal analysis and temperature dependency of embryonic elongation in *Caenorhabditis elegans*

Y. RABIN* & B. PODBILEWICZ†
* *Department of Mechanical Engineering, Technion – Israel Institute of Technology, Haifa 32000, Israel*
† *Department of Biology, Technion – Israel Institute of Technology, Haifa 32000, Israel*

Key words. *Caenorhabditis elegans*, confocal microscopy, elongation, embryos, experimental apparatus, green fluorescent protein, membrane fusion, morphogenesis, temperature control, thermal analysis, time-resolved microscopy.

Summary

A new experimental apparatus for temperature-controlled microscopy has been developed for the study of the temperature dependency of developmental processes in the nematode *Caenorhabditis elegans*. However, the application of this apparatus is rather general and can be used for a wide range of temperatures between −10 and 90 °C. The new apparatus is easy to use, inexpensive, simple to construct, and is designed for precise temperature control of oil-immersion microscopy using epifluorescence. Thermal analysis of the experimental apparatus shows the effects of each of its components, as well as the effects of uncertainty in temperature measurements. Finally, results of this study indicate that: (i) embryos incubated and imaged at temperatures of 8 °C and below do not elongate; (ii) the initial elongation rate is strongly temperature-dependent between 9 and 25 °C.

Introduction

Low temperature is a well-known inhibitor of biological processes involving membranes (Palade, 1975; Blumenthal *et al.*, 1987; Beckers & Rothman, 1992; Podbilewicz & Mellman, 1992). Obviously, means for temperature-controlled microscopy are required for studies involving intact cells, tissues or organisms. A reliable method to image these biological processes at different temperatures is required, in order to study the temperature dependency of the processes of embryonic elongation (Priess & Hirsh, 1986) and cell-to-cell membrane fusion during embryonic and post-embryonic development in *Caenorhabditis elegans* (Podbilewicz & White, 1994). For example, a transgenic *C. elegans* strain expressing MH27-GFP fusion protein (Mohler *et al.*, 1998) can be used to determine the temperature dependency of elongation of *C. elegans* embryos *in vivo*, and time-lapse 4D movies at different temperatures using confocal microscopy can be made.

Temperature-controlled microscopy is well reported in the literature in the context of cell biology, where a recent comprehensive review by Rieder & Cole (1998) focuses on perfusion chambers for living cells. In general, temperature-controlled microscopes for wide temperature ranges and applications are commercially available, but are typically characterized by a very high cost. The controlled temperature can vary from −196 °C (the LN_2 boiling temperature) up to 1500 °C (for example, THMS 600 and TS 1500 temperature stages, respectively, of Linkham Scientific Instruments, Ltd, U.K.).

A new experimental device for temperature-controlled microscopy is presented here. This device has been developed to study the temperature dependency of the elongation rate and cell-to-cell fusion rate of the nematode *C. elegans*. Among others, the applications of this device include reversible anaesthesia of animals using temperatures between 4 and 8 °C, heat and cold shock experiments, and slowing down of biological processes to facilitate imaging in living cells, tissues and embryos. The new device is designed for precise temperature control of oil-immersion microscopy using epifluorescence. Thermal analysis of the experimental apparatus is presented. Finally,

Correspondence: Dr Yoed Rabin, Department of Mechanical Engineering, Carnegie Mellon University, 5000 Forbes Avenue, Pittsburgh, PA 15213, U.S.A. Fax: + 1 412 268 3348; e-mail yoed.rabin@andrew.cmu.edu

© 2000 The Royal Microscopical Society

results indicate that morphogenesis is a temperature-dependent process, where the initial elongation rate of the nematode *C. elegans* is blocked below 8 °C.

Materials and methods

Experimental set-up

The experimental apparatus comprises four main components: (i) a standard temperature-controlled water bath, (ii) a temperature stage, (iii) a microscope lens heat exchanger, and (iv) a temperature measurement unit, as shown in Fig. 1.

The cooling mechanism is a standard temperature-controlled water bath. The water bath used in this study was a LKB 2209, having a working fluid capacity of 3 L, a circulation pump generating a flow rate of up to 10 L min^{-1} and a temperature controller with a temperature resolution of 0.1 °C. Water is suitable as a working fluid for working temperatures above 0 °C, while 50% methanol is suitable for subzero temperatures. A Nikon Eclipse E800 microscope coupled to a BioRad MRC1024 laser confocal scanning microscope, and a Nikon objective lens Planachromat 60× NA = 1.4 and W.D. 0.21 mm, were used in this study. For imaging, the 488 nm line of a 100 mW argon laser was used with neutral density filters to achieve 0.3% of the intensity. The measured power at the output of optical fibre combiner was 73 μW. Interestingly, Tsien & Waggoner (1995) calculated the optimal power to be 76 μW at 488 nm with the best signal-to-noise ratio with respect to autofluorescence and scattering.

Figure 2A shows a horizontal cross-section of the temperature stage at its mid-height. The temperature stage is machined to form a long, narrow, winding tube, which leads the working fluid back and forth along the temperature stage. The winding configuration forces high heat transfer by convection between the working fluid and the stage's internal walls. The stage is made of copper, which is characterized by a very high thermal conductivity, in order to ensure a uniform temperature distribution of the stage surface. The temperature stage is placed on a flat thermal insulator (Plexiglas), in order to reduce heat conduction from the stage to the microscope's base (Fig. 1).

Figure 2(B) shows the microscope lens heat exchanger. Plastic (PVC) was chosen as a construction material for the lens heat exchanger, in order to prevent possible mechanical stress on the lens due to thermal contraction of the heat exchanger. From heat transfer considerations, the thickness of the inner wall between the lens and the working fluid has to be as thin as possible to decrease thermal resistance to heat transfer. Furthermore, the outer wall has to be thick, in order to decrease heat transfer from the surroundings. Regardless of the lens diameter, wall thicknesses of 2 and 5 mm, respectively, are deemed suitable for this purpose when using plastics as construction materials.

With reference to Fig. 1, the microscope lens heat

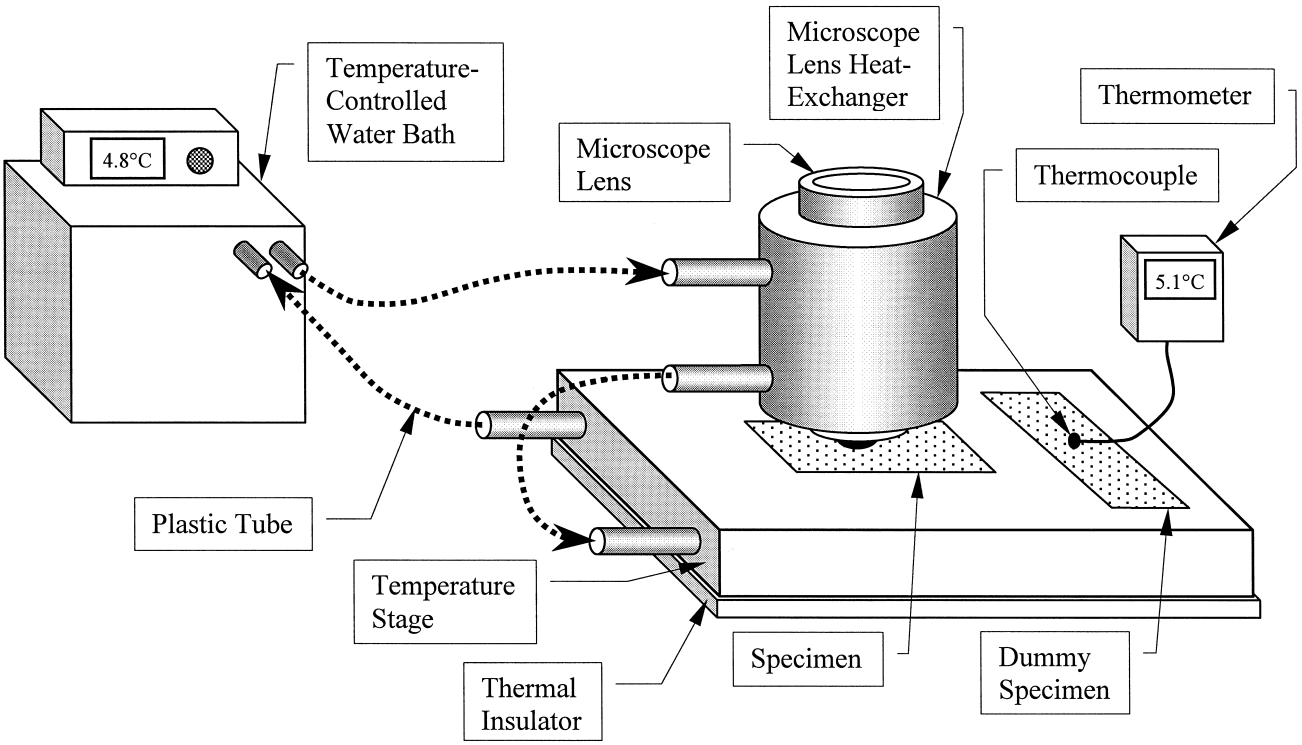

Fig. 1. Schematic illustration of the experimental set-up for temperature-controlled microscopy.

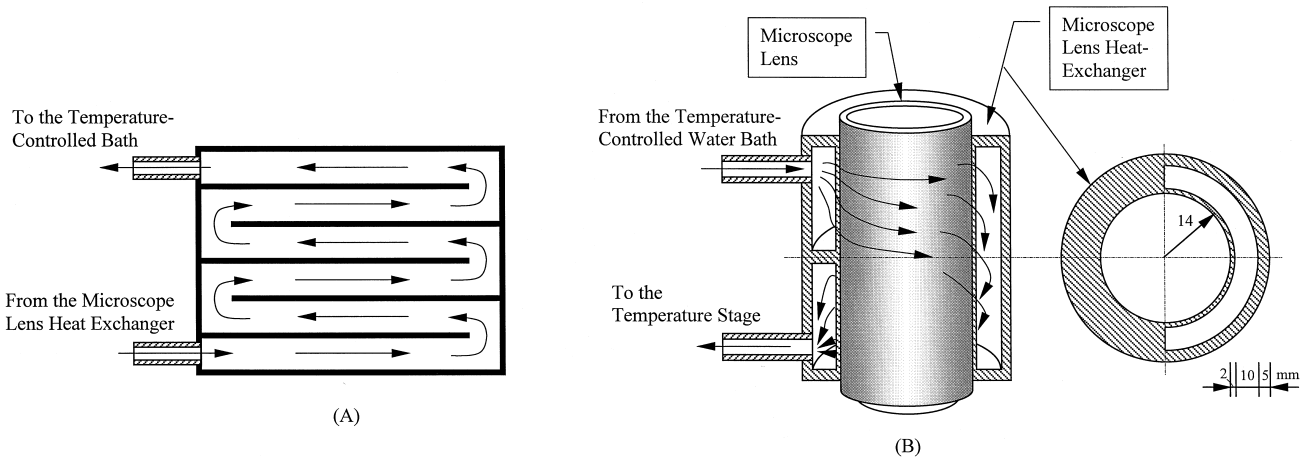

Fig. 2. (A) Horizontal cross-section of the temperature stage. The overall dimensions of the stage are 70 × 100 mm; the working fluid tube is 10 mm wide and 6 mm high; all internal walls are 1.5 mm thick; and the thermal insulator has a thickness of 5 mm (the arrows represent the fluid flow direction). (B) Cross-section of the microscope lens heat exchanger. This heat exchanger is designed in a cylindrical-shell configuration having a flow separator at its mid-height, forcing the working fluid to flow around the lens.

exchanger and the temperature stage are connected by 8 mm plastic (Tygon) tubes, in series, to the external pump of the water bath. The controlled variable of the system is the temperature of the working fluid within the bath. However, because some undesired heat transfer takes place along the tubing, from the working fluid to the surroundings, and to the microscope body, the surface temperature of the temperature stage is different from that of the water bath temperature. Hence, a temperature measurement unit is applied to monitor the actual working surface of the temperature stage, to provide a means for tuning. A standard T-type thermocouple having a diameter of 0.1 mm, and a digital thermometer from Tegam Co. (Geneva, OH, U.S.A.) model 875C were used for the current experimental apparatus.

Nematode strains

Maintenance of nematode strains in the current study was as described by Brenner (1974). To analyse the temperature dependency of embryonic elongation in living embryos a transgenic strain jcIs1 was used, expressing JAM-1 fused to a Green fluorescent protein (GFP) in all adherens junctions (Mohler *et al.*, 1998). MH27-GFP, also called JAM-1, is localized to the adherens junctions as revealed by the monoclonal antibody MH27 (Francis & Waterston, 1991; Podbilewicz & White, 1994; Mohler *et al.*, 1998). jcIs1 strain was grown at 20 °C and early embryos were obtained by cutting hermaphrodites in egg buffer (Edgar, 1995). Embryos were maintained at the experimental temperature for at least 30 min before the onset of elongation.

GFP imaging and length measurements

To measure changes in length during elongation, embryos were placed on round polylysine-coated coverslips in egg buffer (Edgar, 1995). A thin layer of high vacuum grease was applied surrounding the round coverslip, and a 24 × 24 mm coverslip was placed on top ensuring that no air bubbles remained between the two coverslips. For each data time point, optical sectioning and projections of whole embryos were obtained using confocal microscopy and Lasersharp software by BioRad (Podbilewicz, 1996). 4D-time-lapse movies were obtained and the length of the head was measured in individual projections using NIH-Image (freely available from www.scioncorp.com). After the desired temperature was reached the system was stable for up to 15 h of automated time-lapse recording. No problems with vibrations from the moving liquid and with focus drift were found in the system. It has been previously shown by Priess & Hirsh (1986) that the elongation rate of the body is proportional to the elongation rate of the head. The length of the head is defined in this study as the linear distance between the anterior tip of the embryo to the adherens junction between the hypodermal lateral seam cells V1 to V2 and the dorsal junction between cells 6 and 7 of hyp7 (Podbilewicz & White, 1994). The data in Fig. 7 represent single embryos incubated at the specified temperatures. To date, we have imaged 127 wild-type embryos from 4 to 30 °C.

Results

Thermal analysis

Figure 3A shows schematically the cross-section of the experimental apparatus along the centre-line of the microscope lens. The overall distance between the microscope lens and the upper surface of the temperature stage is up to

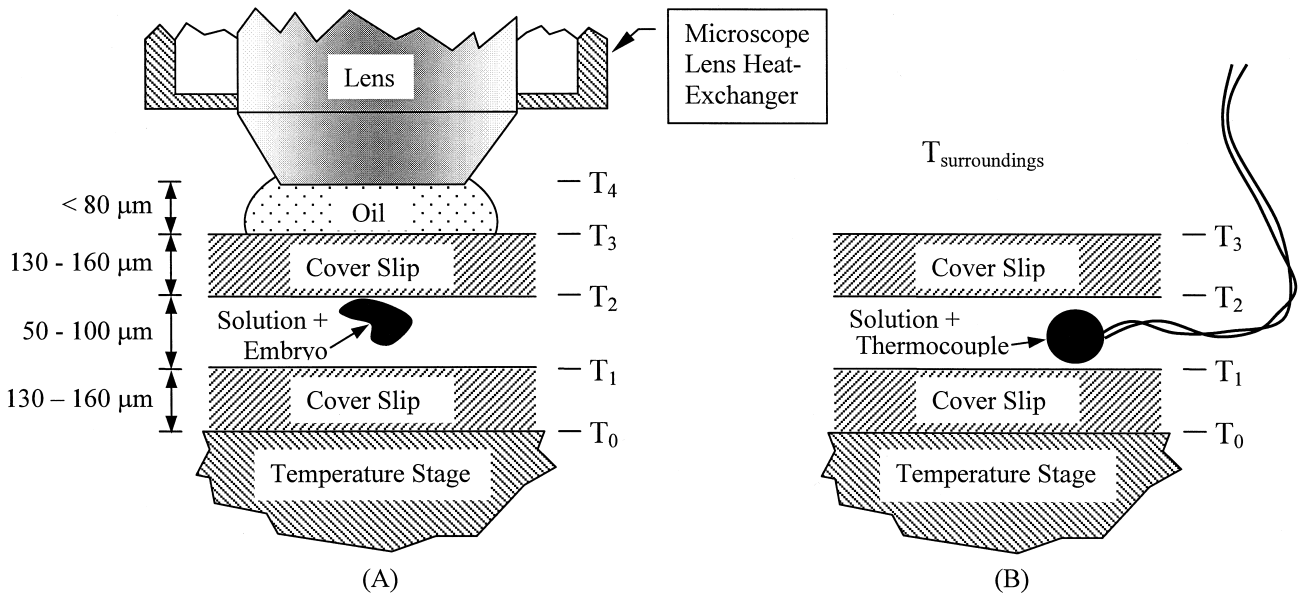

Fig. 3. Thermal models of (A) the lens–temperature stage thermal system, and (B) the thermocouple set-up.

0.5 mm, which is two orders of magnitude smaller than the width of the microscope lens (14 mm O.D.). This indicates that a one-dimensional thermal analysis, along the lens axial direction, is adequate for the current study. In order to demonstrate the necessity in the application of a microscope lens heat exchanger, we first analyse the case of temperature control with a temperature stage but with no lens heat exchanger.

Owing to the high thermal conductivity of the metallic case of the microscope lens and its wide cross-section area, and in the absence of the lens heat exchanger, one may assume the lens temperature to be at room temperature, i.e. in the range 18 to 22 °C. It follows that a temperature variation between room temperature and the stage's temperature is expected to occur over a relatively short distance. For example, for a room temperature of 20 °C, a stage temperature of 0 °C, and the dimensions shown in Fig. 3A, an average temperature gradient in the range 0.020 to 0.035 °C μm^{-1} is expected to develop. Of course, local temperature gradients may be significantly higher, depending on the thermal conductivity of the specific layer; for example, 0.045 °C μm^{-1} in the solution layer, and 0.180 °C μm^{-1} in the oil layer, for the above parameters. It follows that an embryo having a typical thickness of 30 μm will experience temperature differences of 1.5 °C. However, with respect to the stage temperature, the uncertainty regarding the absolute temperature of the embryo is about 6.5 °C for the same example. This observation necessitates a more precise analysis of temperature distribution in the vicinity of the specimen, which dramatically affects the outcome of this study, as addressed below.

Assuming heat transfer solely by conduction between the lens and the temperature stage, and a steady-state condition as a limiting case, one should expect a linear temperature distribution within each layer (Fig. 3). The interface temperature defined in Fig. 3 can be calculated from the following heat flux balance:

$$q'' = k_{ij}\frac{T_i - T_j}{\Delta x_{ij}} \tag{1}$$

where k_{ij} is the thermal conductivity between interface i and

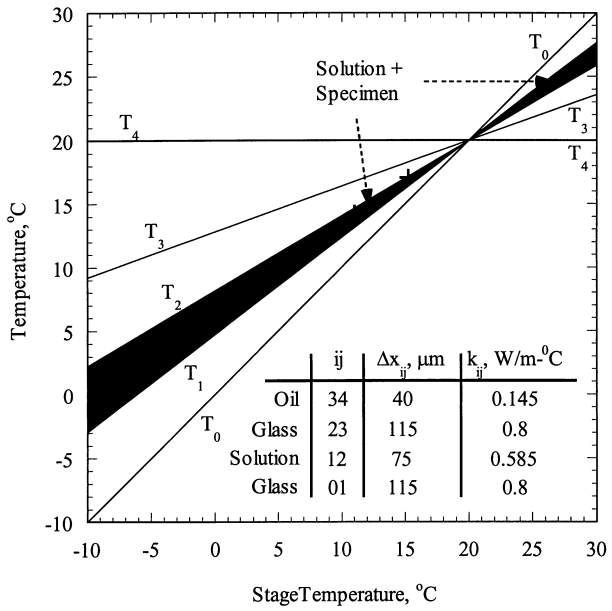

Fig. 4. Interface temperature as a function of the temperature-stage temperature for the experimental set-up shown in (A) calculated by Eq. (1). The grey area represents the solution layer.

the adjacent interface j, Δx_{ij} is the thickness of the layer, T_i is the temperature of interface i, and q'' is the heat flux from the lens to the temperature stage. Typical thicknesses of the various layers in the current study are shown in Fig. 3A.

Figure 4 shows a numerical example of the solution of Eq. (1) for average thickness of the layers specified in Fig. 3(A), and for stage surface temperature in the range -10 to 30 °C, where the lens temperature is kept at an ambient temperature of 20 °C (in the absence of the lens heat exchanger). The typical thermal conductivity values of glass, water and oil, are also shown in Fig. 4. The grey area between T_1 and T_2 curves represents the solution layer between the coverslips.

The following conclusion can be drawn from Fig. 4. (i) The solution temperature deviates significantly from the stage temperature, regardless of the thermal efficiency of the temperature stage. For example, the solution temperature is 8 to 13 °C above the stage temperature for a stage temperature of 0 °C, and 4 to 6 °C below the stage temperature for a stage temperature of 30 °C. (ii) Temperature gradients in the solution layer vary in the range of 95 to -30 °C μm^{-1} when the stage temperature varies in the range -10 to 30 °C, respectively. This indicates high uncertainty in the specimen's temperature due to minor uncertainty in the specimen's location within the solution layer. In summary, Fig. 4 indicates the significant heating effect of the microscope lens on the solution layer including the specimen.

In order to verify the data shown in Fig. 4, the following experiment was carried out. The solution temperature was measured using a thin thermocouple (0.1 mm in diameter), which was inserted into the solution layer shown in Fig. 3(A). A similar thermocouple was inserted into the solution layer of a similar setup on the same temperature stage, but which was not brought in contact with the lens, Fig. 3(B) (shown also in Fig. 1 as a dummy specimen). The thermal resistance to heat transfer by conduction between the temperature stage surface and the thermocouple shown in Fig. 3(B) (proportional to $\Delta x/k$) is about three orders of magnitude smaller than the thermal resistance of heat transfer by natural convection from the upper coverslip to the surroundings (proportional to $1/h$, where h is the heat transfer coefficient by convection). It follows that the latter thermocouple shows the temperature of the upper surface of the stage with high certainty. The results of this experiment are represented by + symbols in Fig. 4, which fall within the calculated solution layer temperature. When evaluating these results, one should bear in mind that the data for Fig. 4 were calculated based on the average values discussed above. Furthermore, the thermocouple junction is not small enough to capture temperature variations within the solution layer but only the average temperature of this layer. However, the experimental data indicate a similar trend of the solution temperature dependency with respect to the stage temperature.

Where the lens temperature equals that of the stage's temperature there is a zero heat flux across the solution layer, Eq. (1), and a uniform temperature distribution between the lens and the stage. This conclusion has prompted us to design the current experimental apparatus, where the lens and the stage are temperature-controlled by the same means and to the same target temperature.

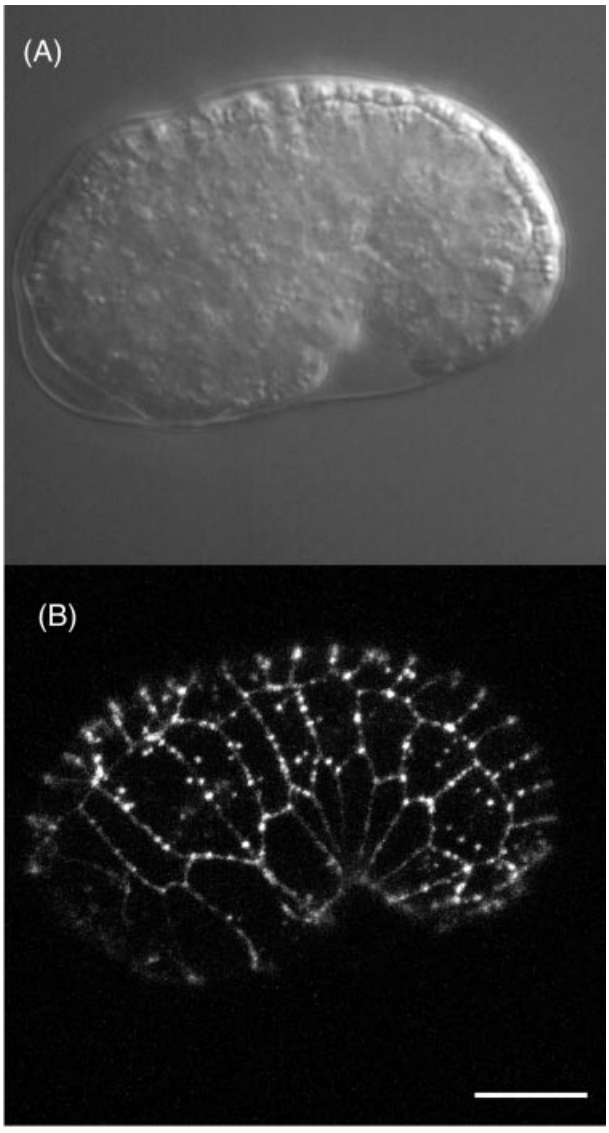

Fig. 5. Living embryo prior to the comma stage ($t = 0$). This embryo was imaged using the MRC1024 confocal microscope showing Nomarski differential interference contrast microscopy (A) and (B) revealing the fluorescent MH27-GFP at the adherens junctions of the epithelial monolayer that forms the hypodermis. Top row of cells is the dorsal hypodermis, middle is the lateral seam cells and bottom cells are the ventral hypodermis (left view) Bar = 10 μm.

When measuring the temperature of the stage's surface one should pay special attention to the manner in which the temperature sensor is attached. For example, when using a thermocouple and attaching it perpendicular to the stage's surface, thermal interaction between the sensor and the sensed phenomenon may dramatically increase uncertainty in measurements (Rabin, 1998a). The uncertainty level can be significantly decreased by attaching the end portion of the thermocouple, not just its tip, to the stage's surface. Alternatively, the working fluid temperature can be measured at the stage's inlet and/or outlet. In this case, a long enough portion of the thermocouple has to be inserted into the tube in the upstream direction, as discussed by Rabin (1998b). Either way, using a copper–constantan thermocouple (Type T) introduces an uncertainty temperature interval of ± 0.5 °C due to the quality of the thermocouple wires, in the working temperature range of interest for the current study.

Temperature dependence of embryonic elongation in C. elegans

Morphogenesis in the nematode *C. elegans* transforms the shape of the embryonic body from a ball of cells into a worm that will hatch after elongating fourfold (Sulston *et al.*, 1983; Priess & Hirsh, 1986). The cells responsible for the elongation of the embryo have been identified as the hypodermal cells that form the outermost epithelial layer surrounding the embryo (Priess & Hirsh, 1986; Sulston *et al.*, 1983). The 78 major hypodermal cells enclose the embryo before it elongates and are arranged in five rows of cells linked together by adherens junctions completely surrounding the embryo (Priess & Hirsh, 1986; Podbilewicz & White, 1994; Williams-Masson *et al.*, 1997). Circumferentially orientated actin fibres within the hypodermal cells contract, squeezing the embryo circumferentially (Priess & Hirsh, 1986; Williams-Masson *et al.*, 1998). As the shape of the hypodermal cells changes, the embryo elongates. Recent work has shown that a catenin–cadherin system (Costa *et al.*, 1998) and a β-spectrin (McKeown *et al.*, 1998) are required for normal elongation of the embryo. Many biological reactions have been studied at different temperatures to determine their optimal conditions, in order to find a temperature that may block the process, to facilitate the work with temperature-sensitive mutants and to analyse the rate limiting step of a multi-step process. It is known that embryonic and postembryonic growth of *C. elegans* is optimal at 20 °C. At 25 °C, growth is about 1.3 times faster than that at 20 °C and 2.1 times faster than that at 16 °C (Hirsh & Vanderslice, 1976; Lewis & Fleming, 1995). Figure 5 shows a living embryo before elongation ($t = 0$); the dorsal hypodermal cells are on the top, and the anterior part of the embryo is to the left. Images and length measurements were obtained every 2–15 min for a total duration of 80–900 min depending on the incubation temperature, which was between 25 and 8 °C. Each time point is the projection of 10–20 confocal images of embryos expressing the MH27-GFP reporter protein at all adherens junctions. Intermediate imaged embryos for three different temperatures are shown in Fig. 6. The initial rate of elongation was linearly calculated from the slope of the curves shown in Fig. 7A. The initiation ($t = 0$) was defined as the comma stage (Priess & Hirsh, 1986; Podbilewicz & White, 1994) and a lag phase before the onset of elongation was observed (Priess & Hirsh, 1986; B.P., unpublished results). The head length was measured until the embryonic muscles started to twitch, which corresponds to about 1.6-fold of elongation. This initial stage of elongation takes about 40 min at 25 °C, while full elongation to fourfold embryos takes 130 min at the same temperature (Sulston *et al.*, 1983; Priess & Hirsh, 1986).

To determine the lowest temperature that allows embryonic elongation, groups of comma stage embryos ($t = 0$) were incubated at different temperatures between 4 and 10 °C and scored for the presence or absence of elongation after 900 min. When embryos were grown and imaged at or below 8 °C, elongation was stopped completely and the dorsal hypodermal cells did not fuse, as revealed by the presence of the MH27-GFP reporter protein (Fig. 6A; B.P., unpublished results). However, embryos that were grown at 9 ± 0.5 °C developed and initiated elongation normally and started moving at the expected elongation stage, but they arrested at twofold (Fig. 6B; arrows show the length of the head). In summary, we have found a simple method to block early embryonic elongation. Here we show that embryos elongated very slowly at temperatures of about 10 °C when compared with the normal growth temperatures, which are in the temperature range 15 to 25 °C (Fig. 7A). As shown in Fig. 7(B), the initial rate of morphogenesis is a temperature-dependent process; this is indicated by an increase in the rate of elongation of *C. elegans* embryos with the increase of temperature. It was also found that cell fusion events between hypodermal cells took place at the expected stages of elongation, as revealed by the disappearance of the MH27-GFP marker from the junctions of the dorsal cells (e.g. Fig. 6C; B.P., unpublished results). Thus, we have found conditions that allow us to block a universal biological process in intact developing animals and establish that morphogenesis in *C. elegans* is a temperature-dependent process.

Discussion

The observation that the microscope lens behaves like a heat source or heat sink for a stage temperature below or above room temperature, respectively, has already been reported in the literature, some three decades ago. Early attempts to overcome this problem for the case of high temperature applications involved independently regulating

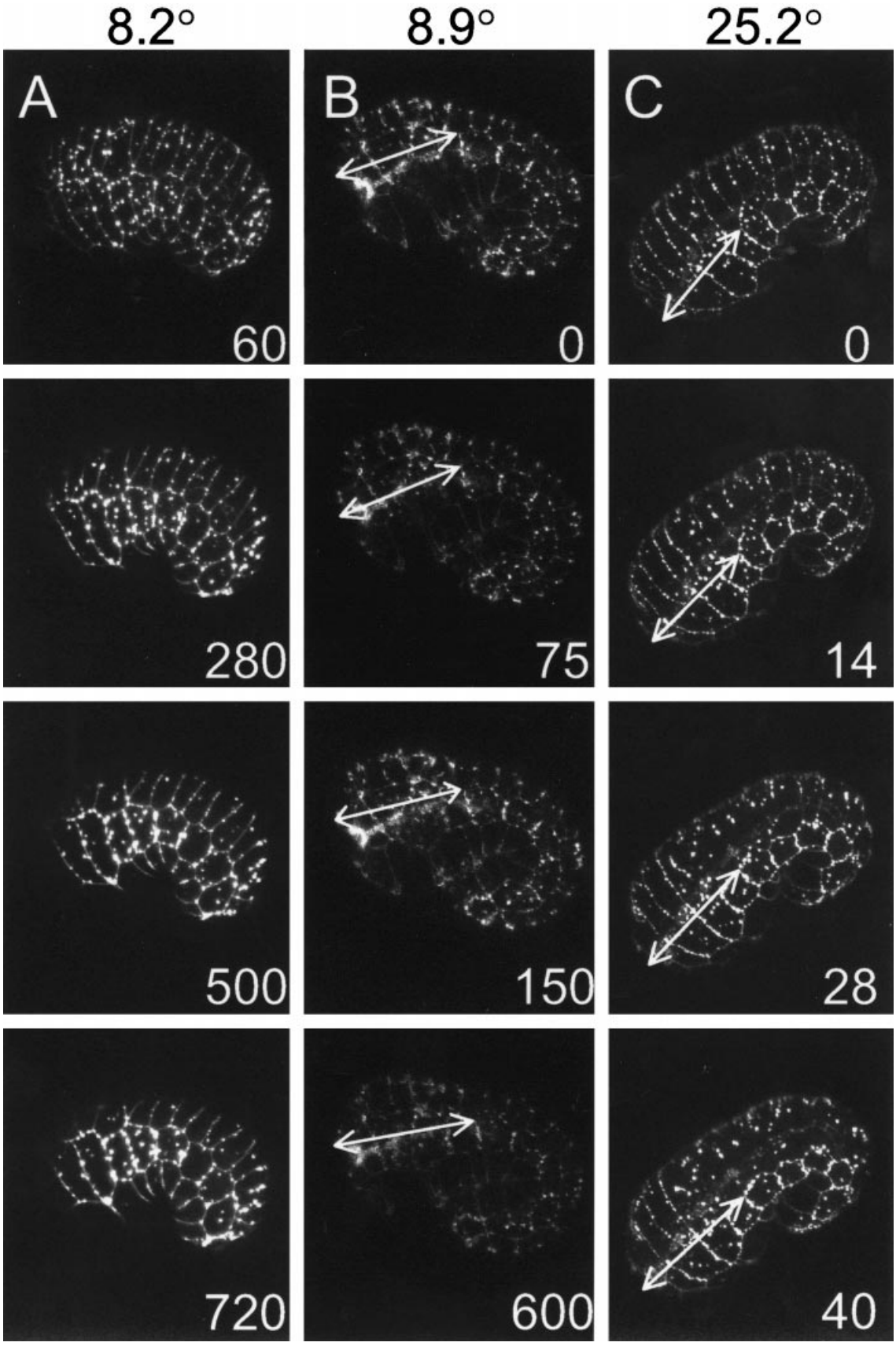
8.2°
8.9°
25.2°
A
B
C
60
0
0
280
75
14
500
150
28
720
600
40

the temperature of the lens with a heating collar (Rieder & Bajer, 1977; Inoue & Spring, 1997). A simpler and more popular solution is to use a heating element and fan to blow air of the desired temperature across the lens (Soll & Herman, 1983). Either way, a second closed-loop control system is required to control the lens temperature. Hence, even when setting the target temperatures of both the stage and the lens to the same prespecified value, temporary differences between the lens temperature and the stage's temperature are likely to occur due to the simultaneous application of two independent closed-loop systems characterized by different time constants of response. Furthermore, the control of lens temperature by heated air can be applied for applications above room temperature only.

Lambert & Bajer (1977), in a report on the arrest of chromosome movement induced by low temperatures, have suggested the use of a cooling coil for the microscope lens. That study was performed with a perfusion chamber, in the temperature range − 4 to 22 °C. The coolant flow rate was gravity controlled at a rate of 80 mL min^{-1}. Such a low flow rate was found satisfactory for the low NA used (0.65), which was applied in the absence of immersion oil. Lambert and Bajer reported a 2 °C temperature difference within the chamber. Furthermore, the effect of lens cooling was demonstrated to have an average magnitude of 2 °C. When compared with the major thermal effect of the microscope lens reported in the current study, the relatively minor effect reported by Lambert and Bajer is attributed to the absence of immersion oil. No thermal model of that set-up is available and therefore uncertainty was assumed to be in the range 0.5 and 1 °C.

In the current experimental apparatus, the stage temperature and the lens temperature are controlled in series by the same means, using a single control variable, which ensures a uniform temperature distribution everywhere between the lens and the stage. The large water bath volume and the high coolant flow rate ensure stable operation: typical temperature fluctuation is 0.5 °C, and typical time of fluctuations is of the order of 1–2 min.

An alternative manner of controlling the specimen temperature is to place the entire microscope system in a temperature-controlled environment, where the surrounding temperature (room temperature) and the desired specimen temperature are the same (Tilney & Porter, 1967; Rieder & Borisy, 1981; Hiraoka & Haraguchi, 1996; Inoue & Spring, 1997). Of course, this is convenient for long-term operations for a relatively narrow range of temperatures. Furthermore, the preparations for microscopy studies in this case are relatively long, as the entire environment has to stabilize to the desired temperature.

The application of perfusion chambers for temperature-controlled studies is widely accepted by cell biologists (Rieder & Cole, 1998), there a specific environment for a particular study may be maintained by controlling the composition of the surrounding solutions as well as their temperature. However, the *C. elegans* embryo is very weakly affected by the surrounding solution in the early stages of development, which is the time period of the *in vivo* study reported here. Furthermore, perfusion may cause the embryo to bounce, vibrate, or even drift, causing difficulty in long-term observations. Hence, the simple temperature stage, with no perfusion chamber, is the preferred choice in our study, and is traditionally applied for nematode studies (Hird, 1996; Mohler & White, 1998; Mohler *et al.*, 1998). The thermal analysis presented above is related to a simple temperature stage with no perfusion chamber, and for illumination from above. This analysis can be taken as a limiting case for the application of a perfusion chamber. In general, the specimen temperature will always be closer to the stage temperature in a perfusion chamber than that predicted in the absence of perfusion. The higher the perfusion rate, the closer is the specimen temperature to the stage temperature. However, this analysis cannot be applied in the case of transmitted light in a perfusion chamber, which requires different thermal modelling.

Previous studies in *C. elegans* embryos have measured embryonic elongation at 20 °C and 25 °C (Sulston *et al.*, 1983; Priess & Hirsh, 1986; McKeown *et al.*, 1998). The rate of body elongation at 25 °C was 2.5 times that of head elongation (Priess & Hirsh, 1986). We calculated initial rates of elongation from the published data and found them to be similar to the rates obtained in the present study. The

Fig. 6. Living transgenic embryos expressing MH27-GFP observed by confocal microscopy. Frames from time-lapse 4D-confocal microscopic reconstruction of MH27-GFP expressing embryos. (A) The four frames in the first column show an embryo that developed at 8.2 °C under the microscope. The arrest phenotype shows no elongation beyond the comma stage and all the dorsal hypodermal cells (top row) remained unfused. (B) Embryo grown at 8.9 °C developed to twofold. This experiment shows that *C. elegans* embryos undergo morphogenesis (elongation) at 9 ± 0.5 °C, start moving at the 1.6-fold stage, and then arrest at the twofold stage. Initial elongation of this embryo was 13 times slower than that at 20 °C. (C) Embryo imaged at 25.2 °C shows a rapid elongation coupled with dorsal hypodermal fusions revealed by the disappearance of the dorsal adherens junctions revealed by the MH27-GFP. Embryos are orientated with the anterior to the left and dorsal side towards the top of the page. The numbers in the lower right corner of each image refer to time points in minutes. The starting time ($t = 0$) is the comma stage, before elongation. The length of the arrows in (B) and (C) represent the length of the head measured from the tip of the head (left end of the arrow) to the junction between the lateral hypodermal cells V1 and V2. The head lengths in μm shown in B (arrows) were 23.9, 25.2, 25.7 and 27.2 μm measured at 0, 75, 150, and 600 s, respectively. Head elongation is proportional to body elongation. The body length increases four-fold at the end of normal embryonic development. Each egg is about 50 μm long.

initial rate of head elongation at 25 °C was 187 nm min^{-1} (Sulston *et al.*, 1983) and 180 nm min^{-1} (Priess & Hirsh, 1986); at 20 °C the initial rate of elongation was 132 nm min^{-1} for both wild-type and *sma-1*(*ru18*) mutant

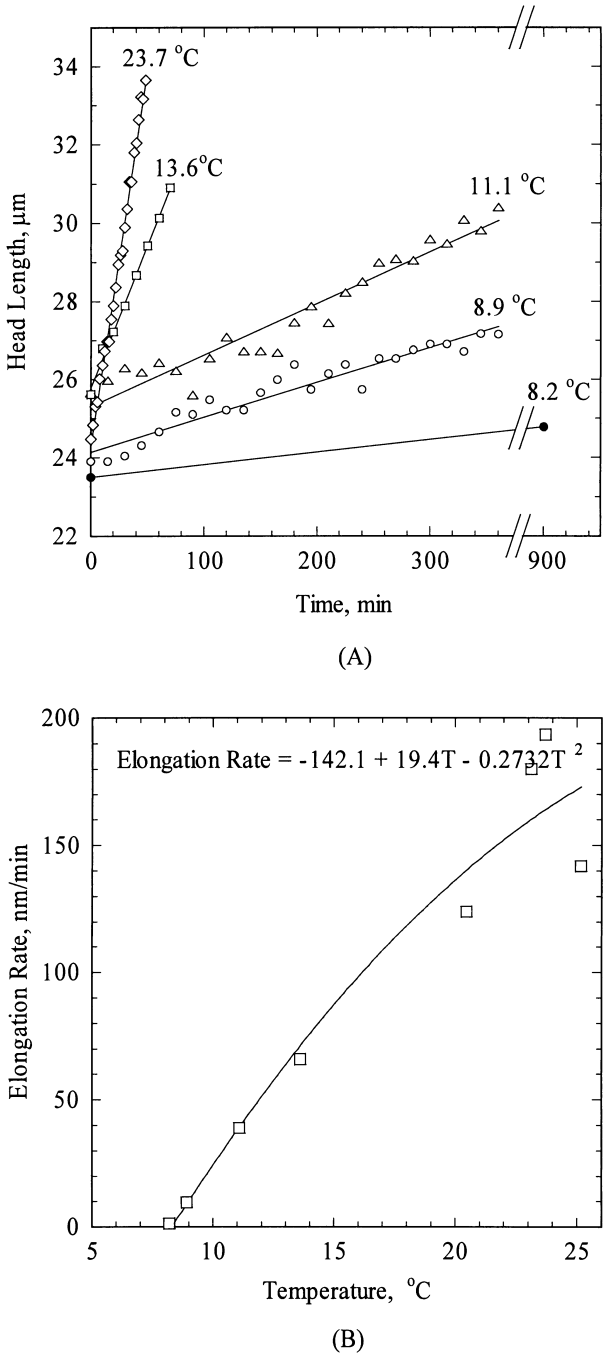

Fig. 7. Temperature dependence of head elongation. (A) The head length of embryos imaged as described in Fig. 6. Each temperature represents data from a single embryo. (B) The slopes of the curves for individual embryos were fitted by linear regression. The correlation coefficient for each temperature was > 0.95. The initial head elongation rate shown here in nm min^{-1} can be multiplied by a factor of 2.5 to get the body elongation rate.

(McKeown *et al.*, 1998). The rates of head elongation calculated after the 1.5-fold stage were found to be two or three times faster than for the initial rates (Sulston *et al.*, 1983; Priess & Hirsh, 1986; McKeown *et al.*, 1998). Moreover, different *sma-1*/spectrin mutations specifically caused a slower rate of morphogenesis (McKeown *et al.*, 1998). As the mutations did not affect the initial rate of elongation it is conceivable that different rate limiting steps are responsible for the initial and the later phases of morphogenesis. A combination of genetic and thermal analysis of morphogenesis in wild-type and mutant embryos will allow a better understanding of the mechanisms of this complex process. The experiments shown here demonstrate the feasibility of using temperature as an inhibitor of morphogenesis to analyse the process of embryonic elongation *in vivo* and to study the temperature dependence of a biological process *in situ*. Similar experiments may be used to reversibly arrest and image intracellular membrane fusion and transport events during endocytosis, exocytosis, cell division cycle and transport across membranes. High temperatures can be used to study the effects of heat-shock on living organisms, tissues or cells. Low temperatures can also be used to slow down developmental and cellular processes, thus allowing imaging of rapidly occurring events in living cells and the analysis of temperature-sensitive mutants.

Acknowledgements

Yoed Rabin acknowledges support of the Stanley Imerman Memorial Academic Lectureship, U.S.A. Benjamin Podbilewicz was supported by the Jacob and Rosaline Cohn Academic Lectureship and by grants from the Israeli Science Foundation, the Israel Cancer Research Fund (U.S.A.) and the Binational Science Foundation (Israel). The authors would like to thank Mrs Miriam Webber for her assistance in preparing this paper.

References

Beckers, J. & Rothman, J. (1992) Transport between Golgi cisternae. *Meth. Enzymol.* **219**, 5–12.

Blumenthal, R., Bali-Puri, A., Walter, A., Covell, D. & Eidelman, O. (1987) pH-dependent fusion of vesicular stomatitis virus with Vero cells. Measurement by dequenching of octadecyl rhodamine fluorescence. *J. Biol. Chem.* **262**, 13614–13619 [erratum appears in *J. Biol. Chem.* **263** (1), 588].

Brenner, S. (1974) The genetics of *Caenorhabditis elegans*. *Genetics*, **77**, 71–94.

Costa, M., Raich, W., Agbunag, C., Leung, B., Hardin, J. & Priess, J.R. (1998) A putative catenin-cadherin system mediates morphogenesis of the *Caenorhabditis elegans* embryo. *J. Cell Biol.* **141**, 297–308.

Edgar, L.G. (1995) Blastomere culture and analysis. *C. elegans:*

Modern Biological Analysis of an Organism (ed. by H. F. Epstein and D. C. Shakes), pp. 303–320. Academic Press, San Diego.

Francis, G.R. & Waterston, R.H. (1991) Muscle cell attachment in *Caenorhabditis elegans*. *J. Cell Biol.* **114**, 465–479.

Hiraoka, Y. & Haraguchi, T. (1996) Fluorescence imaging of mammalian living cells. *Chromosome Res.* **4**, 173–176.

Hird, S. (1996) Cortical actin movements during the first cell cycle of the *Caenorhabditis elegans* embryo. *J. Cell Sci.* **109**, 525–533.

Hirsh, D. & Vanderslice, R. (1976) Temperature-sensitive developmental mutants of *Caenorhabditis elegans*. *Dev. Biol.* **49**, 220–235.

Inoue, S. & Spring, K.R. (1997) *Video Microscopy: The Fundamentals.* 2nd edn. Plenum Press, New York. p. 741

Lambert, A.M. & Bajer, A.S. (1977) Microtubule distribution and reversible arrest of chromosome movements induced by low temperature. *Cytobiologie*, **15**, 1–23.

Lewis, J.A. & Fleming, J.T. (1995) Basic culture methods. *Methods in Cell Biology. Caenorhabditis elegans: Model Biological Analysis of an Organism* (ed. by H. F. Epstein and D. C. Shakes), pp. 3–29. Academic Press, San Diego.

McKeown, C., Praitis, V. & Austin, J. (1998) *sma-1* encodes a βH-spectrin homologue required for *Caenorhabditis elegans* morphogenesis. *Development*, **125**, 2087–2098.

Mohler, W.A., Simske, J.S., Williams-Masson. E.M., Hardin, J.D. & White, J.G. (1998) Dynamics and ultrastructure of developmental cell fusions in the *Caenorhabditis elegans* hypodermis. *Curr. Biol.* **8**, 1087–1090.

Mohler, W.A. & White, J.G. (1998) Stereo-4-D reconstruction and animation from living fluorescent specimens. *Biotechniques*, **24**, 1006–1010.

Palade, G. (1975) Intracellular aspects of the process of protein synthesis. *Science*, **189**, 347–358.

Podbilewicz, B. (1996) ADM-1, a protein with metalloprotease- and disintegrin-like domains, is expressed in syncytial organs, sperm and sheath cells of sensory organs in *C. elegans*. *Mol. Biol. Cell*, **7**, 1877–1893.

Podbilewicz, B. & Mellman, I. (1992) Reconstitution of endocytosis and recycling using perforated Madin-Darby canine kidney cells. *Meth. Enzymol.* **219**, 198–211.

Podbilewicz, B. & White, J.G. (1994) Cell fusions in the developing epithelia of *C. elegans*. *Dev. Biol.* **161**, 408–424.

Priess, J.R. & Hirsh, D.I. (1986) *Caenorhabditis elegans* morphogenesis: the role of cytoskeleton in elongation of the embryo. *Dev. Biol.* **117**, 156–173.

Rabin, Y. (1998a) Uncertainty in temperature measurements during cryosurgery. *Cryo-Letters*, **19** (4), 213–224.

Rabin, Y. (1998b) Uncertainty in measurements of fluid temperature in tubes. *Cryo-Letters*, **19**(5), 319–326.

Rieder, C.L. & Bajer, A.S. (1977) Effect of elevated temperatures on spindle microtubules and chromosome movements in cultured newt lung cells. *Cytobios*, **18**, 201–234.

Rieder, C.L. & Borisy, G.G. (1981) The attachment of kinetochores to the prometaphase spindle in PtK_1 cells: recovery from low temperature treatment. *Chromosoma*, **82**, 693–717.

Rieder, C.L. & Cole, R.W. (1998) Perfusion chambers for high-resolution video light microscope studies of vertebrate cell monolayers: some considerations and design. *Methods Cell Biol*, **56**, 253–275.

Soll, D.R. & Herman, M.A. (1983) Growth and inducibility of mycelium formation in *Candida albicans*: a single-cell analysis using a perfusion chamber. *J. Gen. Microbiol.* **29**, 2809–2824.

Sulston, J.E., Schierenberg, E., White, J.G. & Thomson, J.N. (1983) The embryonic cell lineage of the nematode *Caenorhabditis elegans*. *Dev. Biol.* **100**, 64–119.

Tilney, L.G. & Porter, K.R. (1967) Studies on microtubules in heliozoa. The effect of low temperature on these structures in the formation and maintenance of the axopodia. *J. Cell Biol.* **34**, 327–343.

Tsien, R.Y. & Waggoner, A. (1995) Fluorophores for confocal microscopy. *Handbook of Biological Confocal Microscopy* (ed. by J. Pawley), pp. 267–279. Plenum Press, New York.

Williams-Masson, E.M., Heid, P.J., Lavin, C.A. & Hardin, J. (1998) The cellular mechanism of epithelial rearrangement during morphogenesis of the *C. elegans* dorsal hypodermis. *Dev. Biol.* **204**, 263–276.

Williams-Masson. E.M., Malik, A.N. & Hardin, J. (1997) An actin-mediated two-step mechanism is required for ventral enclosure of the *C. elegans* hypodermis. *Development*, **124**, 2889–2901.